

Estimation of Moment Magnitude (M) for Small Events ($M < 4$) on Local Networks

by Gail M. Atkinson, D. Wesley Greig, and Emrah Yenier

ABSTRACT

We develop a simple model to estimate moment magnitude for events of $M < 4$ at distances out to ~ 300 km, based on readily available ShakeMap parameters and seismological scaling principles. Estimates of moment magnitude for such small events are not available from standard methods but are needed for local-network applications and for traffic light systems for induced-seismicity applications. This issue is currently of particular interest in central and eastern North America. The method takes advantage of the fact that for small events the response spectrum is well-correlated with seismic moment for periods greater than 0.3 s and can be predicted from a simple stochastic point-source model. We develop an equation by which we calculate M from the 1 s pseudoacceleration amplitudes (PSA) ($M \geq 3$) or the 0.3 s PSA ($M < 3$) at each station, using a simple linear equation that corrects for the effects of attenuation. We show that this method produces unbiased estimates of moment magnitudes in both eastern and western North America, for $M \leq 4$ events recorded at distances < 300 km.

INTRODUCTION

This article outlines a simple method to estimate moment magnitude M (Hanks and Kanomori, 1979) for small events ($M < 4$) based on recorded ground-motion parameters from a local seismographic network. The focus here is on small events, as the seismic moment (and hence M) from larger events can be obtained from standard seismological methods using regional and/or global data. For example, global and regional seismic moment tensor solutions are routinely available for most of North America from the University of St. Louis website of R. Herrmann for $M > 3.5$ events (<http://www.eas.slu.edu/eqc/eqcmt.html>; last accessed May 2014) or from the Global Moment Tensor catalog for events of $M > 4.5$ (www.globalcmt.org; last accessed May 2014). The challenge is in determining reliable and robust estimations of size for

small events ($M < 4$), particularly the very small events ($M \leq 3$) that may only be recorded above noise at close distances. Reliable moment estimates are difficult to obtain for such events with either conventional moment estimation methods or with methods based on calibration of regional data. Obtaining reliable moment estimates for small events is an important problem for two common seismological applications: (1) developing magnitude–recurrence relations for regions that merge small-event and large-event seismicity catalogs and (2) for induced-seismicity applications, in which traffic light protocols for responding to induced events require a reliable assessment of moment magnitude. These applications are currently of great interest in central and eastern North America (ENA).

The proposed method is based on vertical-component 5% damped pseudoacceleration amplitudes (PSA) at 1 s or 0.3 s. (PSA at 1 s is defined as the maximum displacement, in response to the ground motion, of a single-degree-of-freedom 5% damped oscillator, having a natural vibration period of 1 s, multiplied by the factor $(2\pi)^2$). Response spectra at 1 s and 0.3 s are commonly used parameters in engineering seismology; for example, both of these are standard ShakeMap parameters (Wald *et al.*, 1999). Moreover, PSA at 1 s and 0.3 s provide a stable estimate of low-frequency ground motion for small events that is closely correlated with seismic moment. Recently, Atkinson and Babaie Mahani (2013) showed that reliable estimates of M may be obtained for moderate events in North America (M 3–5) using PSA at 1 s recorded at regional distances (150–500 km) and a technique that employs calibration to moderate events with known moment magnitude. Although this technique is useful for moderate events, it may not be useable for the small events ($M < 3$) that are particularly important for induced-seismicity applications, because such events may not have adequate signal-to-noise ratio at 1 s at regional distances. Moreover, due to the lack of calibration events with known M , the method would rely on extrapolation of the calibration-based equations beyond the magnitude range in which they were defined and might thus be significantly biased.

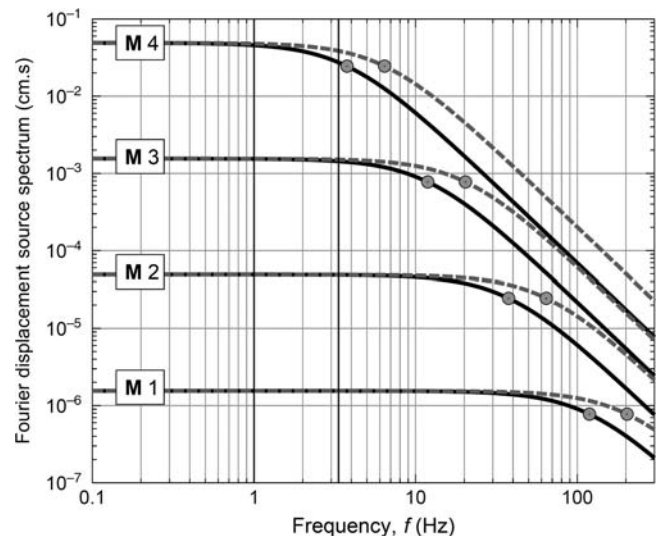
Therefore, we need a modified approach that will make optimal use of local network data over a range of distances from short (<20 km) to regional (<300 km) and that will have a reliable basis when applied to small events for which independent M estimates are not available for calibration. The purpose of this article is to describe such an approach.

METHOD FOR ESTIMATING M FOR SMALL EVENTS

In this study, we develop a robust method of estimating M from PSA at 1 s or 0.3 s from local network data, focusing on short-to-regional distances and using a stochastic point-source model to provide a physically based scaling of the relationship down to small magnitudes. The vertical-component PSA at 1 s (PSA_1) is selected as the preferred parameter for our method; however, as discussed further in the following, we also use PSA at 0.3 s ($PSA_{0.3}$) for small events ($M < 3$) to allow for greater signal-to-noise ratio. We use the vertical component because it minimizes the influence of site response and is applicable to a range of sites, which may have unknown site conditions. In general, vertical-component PSA will be similar to an unamplified horizontal-component PSA (see Lermo and Chavez Garcia, 1993; Siddiqi and Atkinson, 2002; Atkinson and Boore, 2006).

For events of $M < 4$, 1 s is on the flat low-frequency end of a standard Brune (1970) model displacement spectrum, in which the amplitude is directly proportional to seismic moment (Fig. 1). Moreover, for sufficiently small events ($M < 3$), 0.3 s is also on the low-frequency end of the spectrum over a wide range of stress-drop values. We use this basic seismological principle to formulate the method to estimate M . At 1 s, PSA will scale with seismic moment in a manner that is practically independent of stress drop; the same is true for 0.3 s PSA if the event is of $M < 3$. This simple point-source model is appropriate for the small events of interest here and has been shown to be a reasonable model for ground motions in many parts of the world; see Boore (1983, 2003) for examples and a discussion of the seismological principles involved. The response spectrum is similar to a Fourier spectrum, though not identical because the response spectrum shows the maximum response of an oscillator to a record, whereas the Fourier spectrum is a more direct measure of its amplitude at each frequency. Atkinson (2012) shows the relationship between Fourier and response spectral amplitudes for small events in ENA.

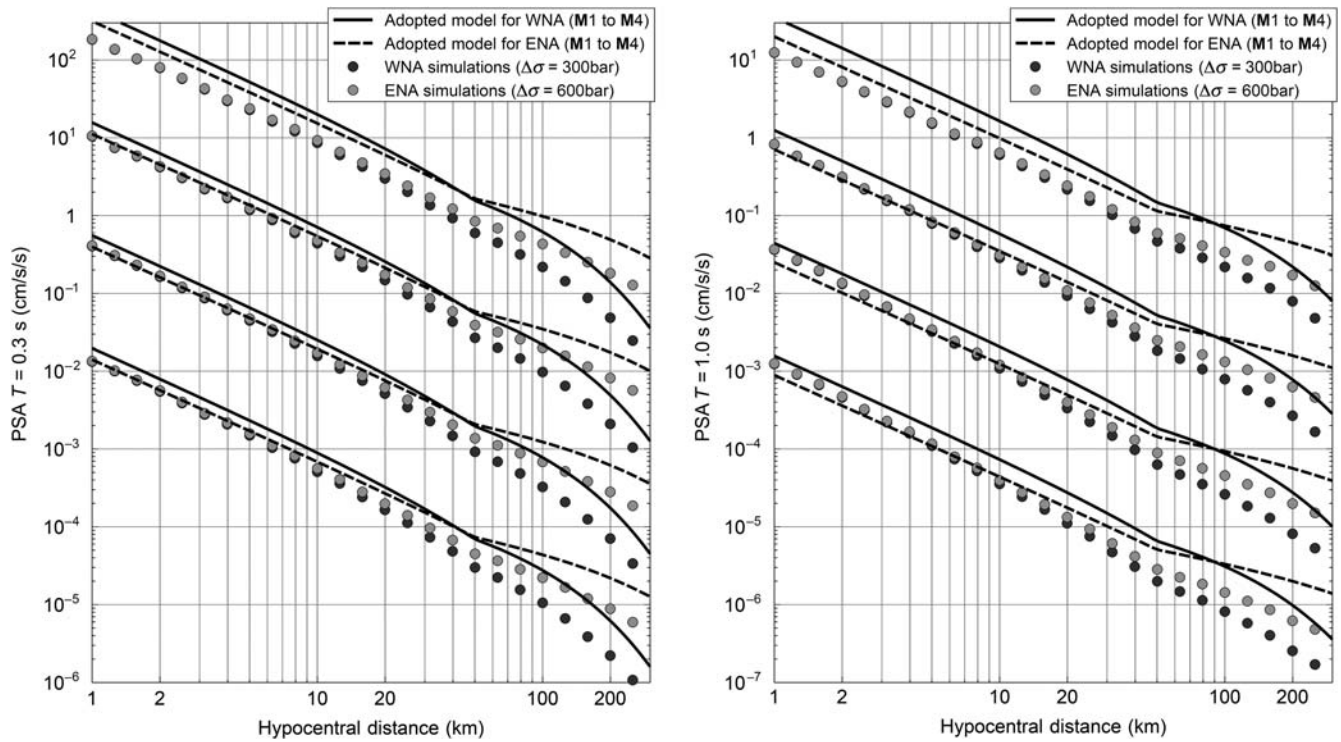
The approach taken is to use a model-driven ground-motion prediction equation (GMPE) for PSA_1 and $PSA_{0.3}$, formulated as a function of M and distance, as a tool from which to calculate M at each station. To do this, we use the stochastic point-source algorithm Stochastic-Method Simulation (SMSIM; Boore, 2000) to simulate time series for M 0–4 events (in increments of 0.2 units) at distances from 1 to 300 km (in increments of 0.1 log units), from which we calculate the average PSA at 1 s and 0.3 s. The model-based GMPE is an equation we define to express PSA_1 and $PSA_{0.3}$ as a simple function of M and the distance to the hypocenter (R).



▲ **Figure 1.** Source spectrum (at $R = 1$ km) for M 1, 2, 3, and 4 for stress-drop values of 100 bars (solid lines) and 500 bars (dashed lines) for the Brune point-source model (neglecting high-frequency effects of κ). Circles show corner frequencies, and vertical black lines highlight 1 Hz (= 1 s) and 3.3 Hz (= 0.3 s).

The underlying assumptions in these predictions, and their justification, are as follows:

1. The vertical component has minimal site amplification, thus no crustal or site amplifications are applied. This is consistent with a simplified interpretation of the relationship of horizontal-to-vertical spectral ratio to site response (Lermo and Chavez-Garcia, 1993; Siddiqi and Atkinson, 2002) and has been applied in previous GMPEs, such as Atkinson and Boore (2006).
2. We assume a hinged bilinear form for the attenuation model, following Babaie Mahani and Atkinson (2012) and Yenier and Atkinson (2014); the geometrical spreading is modeled as $R^{-1.3}$ and $R^{-0.5}$ at distances ≤ 50 and > 50 km, respectively.
3. The stress drop is 300 bars for western regions or 600 bars for eastern regions; these values are consistent with the adopted attenuation models, according to empirical data analyses in the two regions as shown by Atkinson and Boore (2014) for ENA and Yenier and Atkinson (2014) for western North America (WNA).
4. Anelastic attenuation is represented by a whole-path Q , given as $Q = \max(170f^{0.45}, 100)$ for western regions (Raouf *et al.*, 1999) or $Q = 525f^{0.45}$ for eastern regions, in which f is frequency (Atkinson and Boore, 2014).
5. Duration is given by $1/f_0 + 0.05R$ in all regions, in which f_0 is the corner frequency (which depends on moment and stress drop as described by Boore, 2003); the duration model is one that is commonly adopted for point-source simulations (Atkinson and Silva, 2000; Boore, 2003; Atkinson *et al.*, 2009).
6. Near-surface attenuation is represented with the kappa parameter (Anderson and Hough, 1984), assuming



▲ **Figure 2.** The adopted model of vertical-component pseudoacceleration amplitudes (PSA) at (left) 0.3 s and (right) 1 s as a function of hypocentral distance based on Stochastic-Method Simulation (SMSIM) point-source simulations. Points show simulation results, and lines show model defined to represent simulation points after calibration with empirical data (equation 1).

$\kappa_0 = 0.02$ s. This is a typical value for competent sites with minimal site effects (e.g., Atkinson and Boore, 2006; Campbell, 2009).

Figure 2 plots the simulated $PSA_{0.3}$ and PSA_1 amplitudes for both eastern and western attenuation models, along with the function that we have defined as a basis for the magnitude estimation:

$$\log PSA_T = C_T + 1.45M - \log Z(R) - \gamma_T R, \quad (1a)$$

in which T represents period (either 0.3 s or 1 s), C is a constant to be defined, γ the coefficient of anelastic attenuation, and $Z(R)$ is the geometrical attenuation that is given by

$$\log Z(R) = \begin{cases} 1.3 \log R & R \leq 50 \text{ km} \\ 1.3 \log 50 + 0.5 \log(R/50) & R > 50 \text{ km} \end{cases} \quad (1b)$$

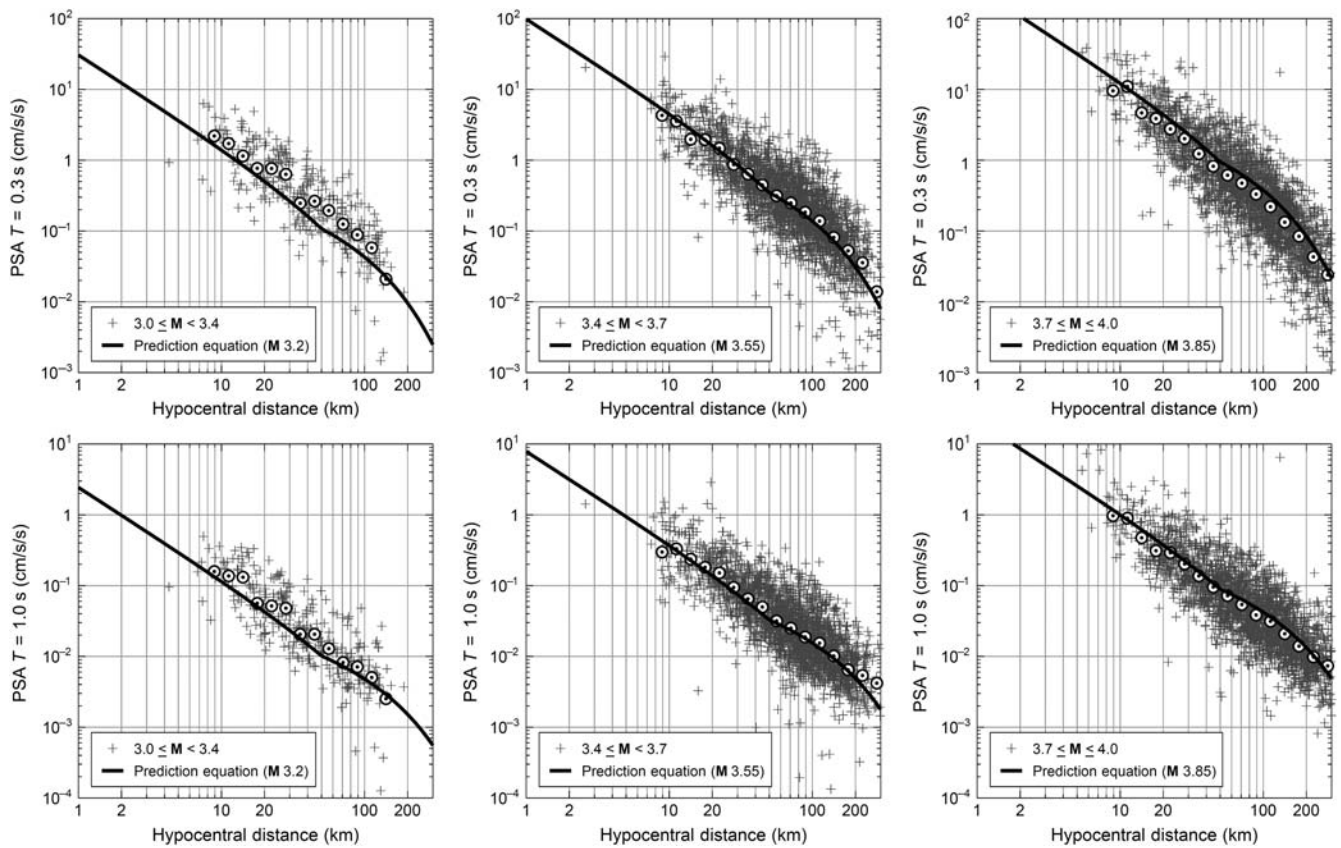
The logarithmic terms are in base 10. R is the hypocentral distance in km, and PSA is in cm/s^2 . Equation (1) employs the same geometrical attenuation model used for the simulations. Table 1 gives the values of the coefficients that correspond to the lines on Figure 2 and which define our adopted ground-motion model that is used in estimation of M .

The equation is very simple, because the scaling of PSA at 0.3 s and 1 s is very regular for small events (Fig. 1); we caution that this equation would generally underestimate M if applied to events of $M > 4$, as it does not consider saturation effects that come into play when modeling larger events as a point

source. The defined lines are not a regression fit to the simulated points, but rather represent the overall trends, in particular the magnitude-scaling indicated by the simulations from M 0 to 4 at typical local-network distances of 5–50 km. The offset of the lines from the simulated values, apparent in Figure 2, reflects an empirical calibration factor that we use to ensure a good fit of the model equations to observations in both WNA and ENA, as discussed in the next section. Essentially, we used the simulations to determine the magnitude scaling that we wished to impose on our ground-motion amplitude model. Then, with the geometric spreading and magnitude scaling held fixed, we calibrated the C_T and γ_T terms based on the empirical ground-motion data (next section) to determine their values, as given in Table 1. We note that if we had simply

Parameter*	Western North America (WNA)		Eastern North America (ENA)	
	0.3 s	1.0 s	0.3 s	1.0 s
C_T	-3.15	-4.25	-3.3	-4.5
γ_T	0.005	0.0035	0.0015	0.0007

* C is a constant and γ is the coefficient of anelastic attenuation for the specified period T .



▲ **Figure 3.** Comparison of equation (1) (lines), evaluated at M 3.2, 3.55, and 3.85, with western North America (WNA) ground-motion data (plus symbols) for PSA at (top) 0.3 s and (bottom) 1.0 s. Circles show average data amplitudes in distance bins.

regressed the simulated amplitudes to obtain the coefficients of equation (1), we would obtain very similar values to those in Table 1, but the constant C would be approximately 0.3 units lower in WNA and 0.1 units lower in ENA for the simulated values. This offset between simulations and observations reflects model misfits attributable to factors such as unmodeled source and site effects and the effect of noise on observed PSA.

In Table 1, we provide variants for two typical regional γ values, which are applicable to active tectonic regions (such as WNA) and stable continental regions (such as ENA). This primarily affects the term in R , though there is also a difference in the constant, due to the calibration to observed regional ground-motion amplitudes. The coefficient in R and the overall constant term can be adjusted where warranted on a regional basis using empirical observations, without affecting the overall magnitude scaling that is constrained by the Brune point-source model.

We invert equation (1) to write an expression to calculate M at a station based on measured PSA_1 or $PSA_{0.3}$:

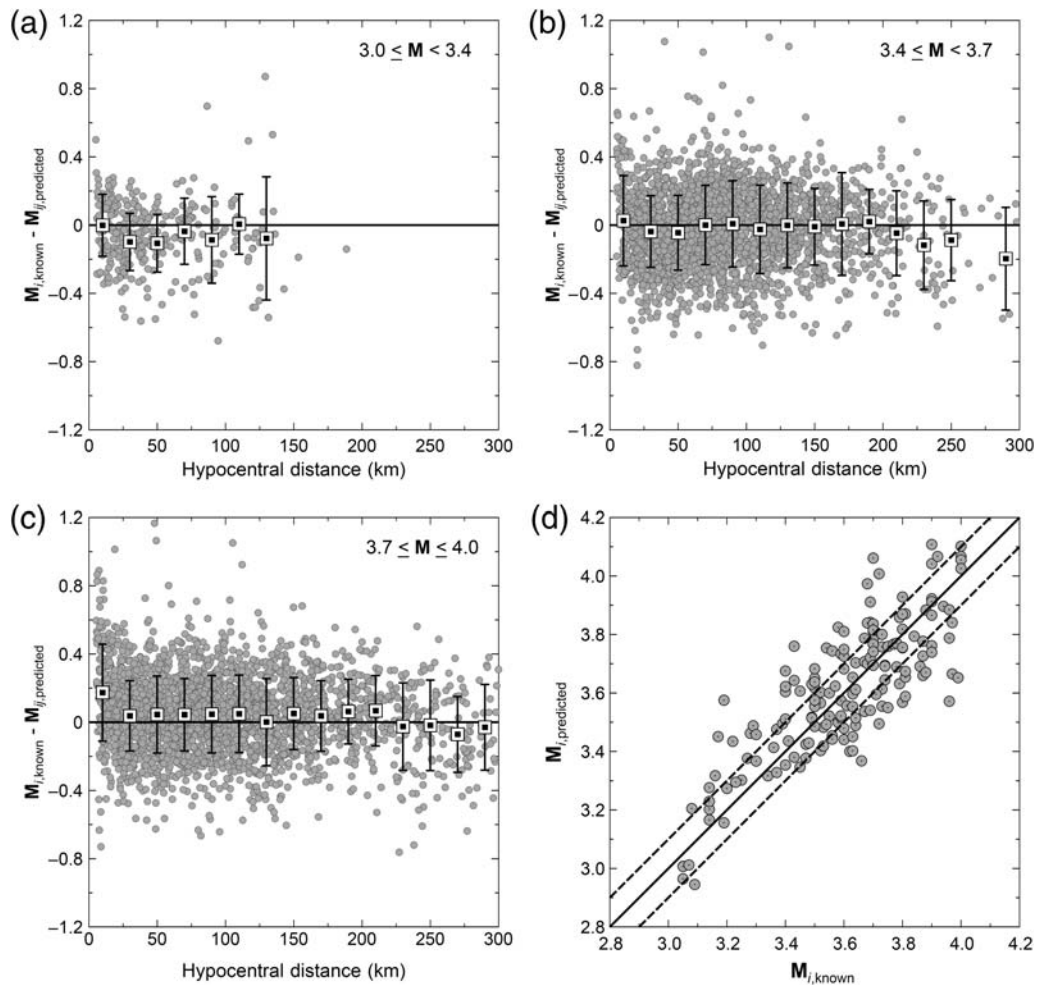
$$M = \frac{\log PSA_T - C_T + \log Z(R) + \gamma_T R}{1.45}, \quad (2)$$

with the coefficients as listed in Table 1. To apply this estimation method to recorded PSA data, we assume that $R = \sqrt{(D^2 + b^2)}$, in which D is epicentral distance and b

is focal depth. For local network applications, we recommend assigning a nominal depth of 5 km to all events to ensure stability. The reason we fix the depth is that it may not be well determined initially; the actual depth value is not critical in this application, as long as it is reasonable (e.g., the magnitude will be relatively insensitive to depth within the range of focal depths from 1 to 20 km). The average M for an event is determined by averaging M estimates obtained over all stations for which we have a reasonable signal-to-noise ratio (e.g., a factor of three).

CALIBRATION AND EVALUATION OF PERFORMANCE

We used ground-motion databases to calibrate the overall level of the M formulation equation and to test its performance. For WNA, we use the Next Generation Attenuation-West 2 (NGA-W2) ground-motion database (www.peer.berkeley.edu; last accessed May 2014), which at small magnitudes is comprised of data from California. Figure 3 plots the data amplitudes of $PSA_{0.3}$ and PSA_1 in comparison to the prediction equations for WNA. It is important to note there are no data in the database for $M < 3$, thus the curves can only be compared to data for events of $M \geq 3$. A small initial mismatch in overall amplitude level between the simulations and the observations was corrected by an appropriate choice of the constant



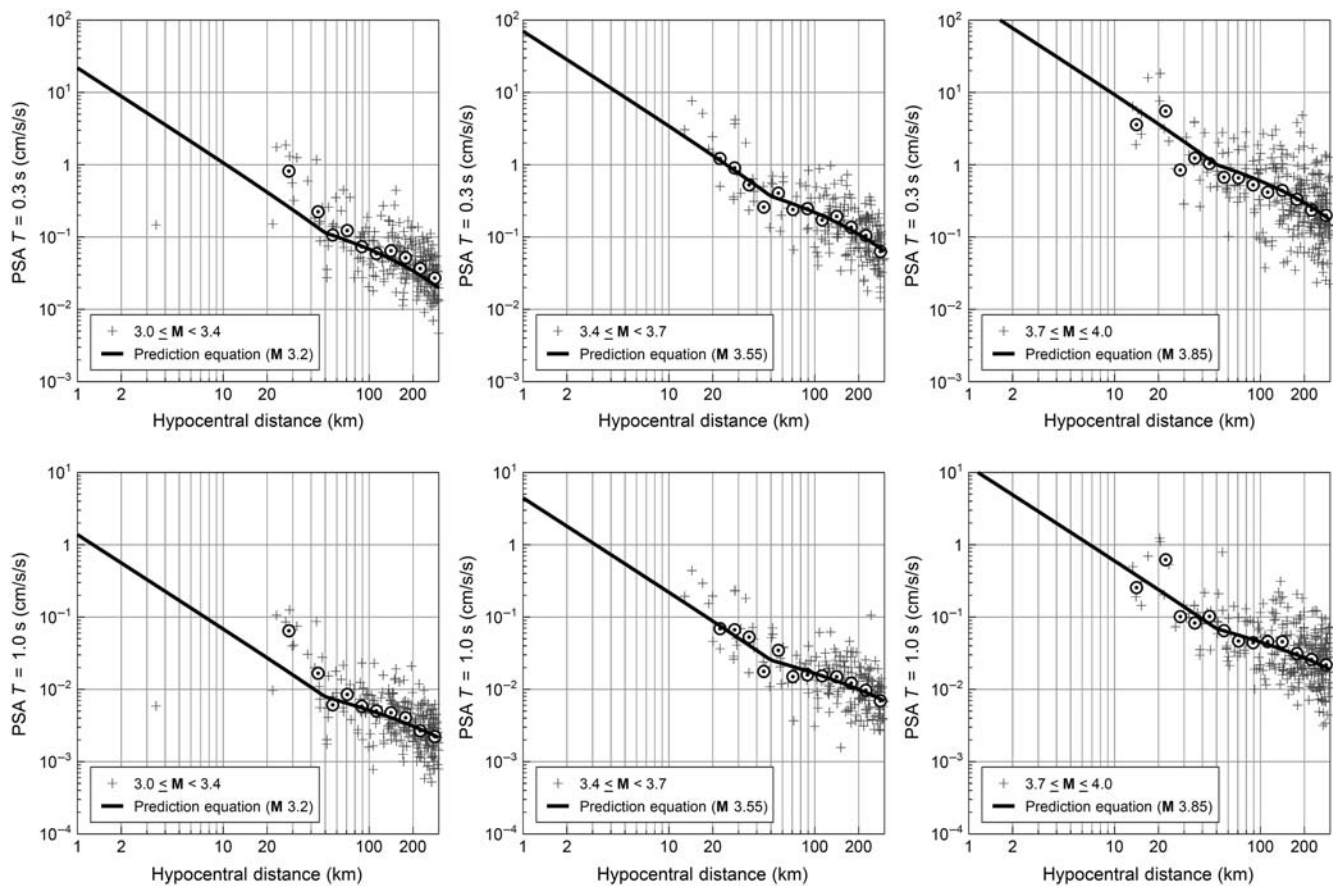
▲ **Figure 4.** Assessment of M estimates (equation 2) based on the ground motions from Next Generation Attenuation-West 2 (NGA-W2) database, showing the M bias determined for each record, as a function of hypocentral distance for three magnitude ranges (a–c). Mean bias is computed over all magnitudes, at equal distance intervals of 20 km. (d) Average M estimate and its known value for earthquakes having three or more observations at $R \leq 300$ km. The solid line represents $M_{i,\text{predicted}} = M_{i,\text{known}}$, and the dashed lines indicate ± 0.1 band about the solid line.

term in equation (1), which is equivalent to applying a calibration factor; this is the source of the offset seen in Figure 2 between the defined prediction lines and the simulation amplitudes. It is interesting that the offset, and hence the calibration factor required, is greater in WNA than in ENA (0.3 log units versus 0.1 units). This may reflect greater site amplification effects that are present on the vertical component in WNA due to the gradational shear-wave velocity profile. Overall, Figure 3 shows that there is good agreement between the observed PSA data and the defined model equations in both amplitude level and attenuation shape, suggesting that the model is generally applicable and that the assumed attenuation is reasonable.

Figure 4 provides a more quantitative evaluation of how well the proposed M estimation model (equation 2) works for the NGA-W2 database. For each observation with $M \leq 4$ and $R \leq 300$ km, we calculate M from equation (2) (with $C = -4.25$ and $\gamma = 0.0035$) and compare it to the known value of M tabulated in the NGA-W2 database to define

the M bias. (e.g., $M_{i,\text{known}} - M_{j,\text{predicted}}$, in which $M_{i,\text{known}}$ represents the known M of event i and $M_{j,\text{predicted}}$ denotes the predicted M for the same event using the PSA obtained at station j). By plotting the bias versus distance in several magnitude ranges, we observe that the equation works well for M 3–4 events at distances up to 300 km, with no significant trends. Moreover, comparing the known M with the estimated values, for earthquakes having three or more observations within 300 km, we note that predictions generally lie within ± 0.1 units of the known magnitude value.

We test the performance of the model for earthquakes in ENA using the NGA-East and seismotoolbox databases, as compiled by B. Hassani and G. Atkinson (2014, manuscript). These data cover the regions of southeastern Canada/northeastern United States and the central United States. (Tests were made to confirm that the noted trends do not differ significantly between the northeast and the central United States.) Figure 5 shows the data amplitudes with respect to equation (1), whereas



▲ **Figure 5.** Comparison of equation (1) (lines), evaluated at M 3.2, 3.55, and 3.85, with eastern North America (ENA) ground-motion data (plus symbols) for PSA at (top) 0.3 s and (bottom) 1.0 s. Circles show average data amplitudes in distance bins.

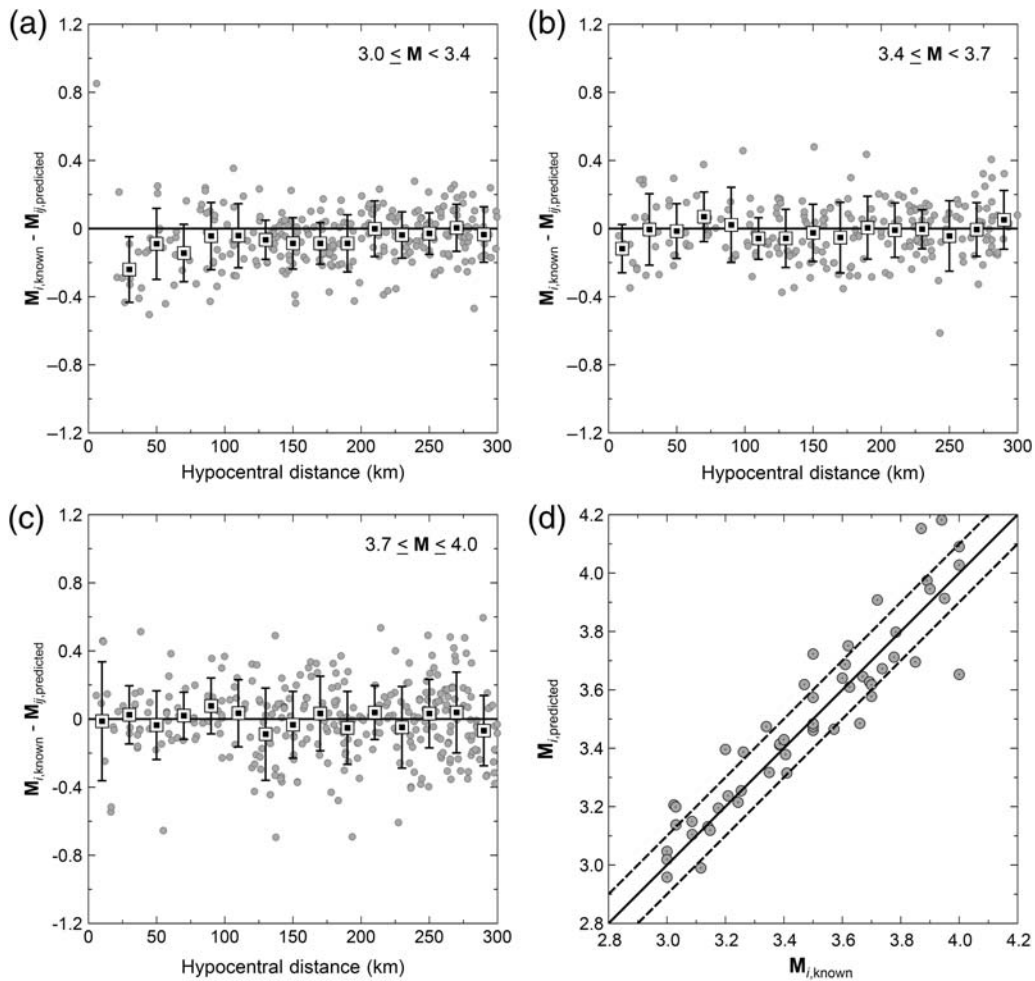
Figure 6 shows the bias in terms of estimated moment magnitude, as well as average M estimates for events in the ENA database (in which the M values are derived from or calibrated to regional moment tensors, as in [Atkinson and Babaie Mahani, 2013](#)). The agreement is satisfactory overall, though in some magnitude ranges there is a tendency for larger-than-predicted amplitudes at close distances. However, the data at close distances are sparse. Average M estimates for earthquakes having three or more observations within 300 km are mostly within ± 0.1 units of the known M , for $M \leq 4$.

MOMENT MAGNITUDE ESTIMATION FOR EVENTS OF $M < 3$

We have shown that the proposed moment magnitude estimation equation based on PSA at 1 s works well in both ENA and WNA, for M 3–4 events at distances up to 300 km. The use of point-source simulations to constrain the magnitude scaling should ensure robust and meaningful magnitude estimates at smaller magnitudes. However, the influence of noise on PSA becomes important for $M < 3$ and could result in a bias toward overestimation of event magnitudes. We examined typical regional network data in eastern and western Canada to determine response spectral amplitudes that would be expected

from noise alone (e.g., oscillator response for a window of 30–60 s in length, in the absence of any earthquake signal). It is common to observe PSA, from noise alone, in the range from 10^{-4} to 10^{-3} cm/s^2 , over a broad period band. As illustrated in Figure 7, this significantly limits the magnitude–distance range over which we can obtain moment magnitudes using PSA at 1 s, because small events will only have significant signal, in relation to the noise PSA, at very close distances. One solution would be to reduce the noise through improved installation techniques, for example by placing instruments in deep boreholes. A more economical and practical solution in most situations is to choose a period band in which the signal for small events is stronger. This is the motivation for using 0.3 s PSA in place of 1 s PSA for $M < 3$ events and why we derived equations using both 0.3 s and 1 s PSA values. Specifically, we observe in Figure 7 that for relatively quiet conditions (the lower noise level), the signal PSA at 0.3 s is above noise for M 1 events within 40 km, whereas for 1 s it is only above noise within 8 km. For $M < 3$ events, the 0.3 s PSA is at a sufficiently long period to represent the moment of the event (Fig. 1), thus it is logical to use the 0.3 s PSA in preference to the 1 s value to improve the signal-to-noise ratio.

As a practical matter, then, we propose that if the magnitude value calculated from the 1 s PSA is < 3 , the magnitude for

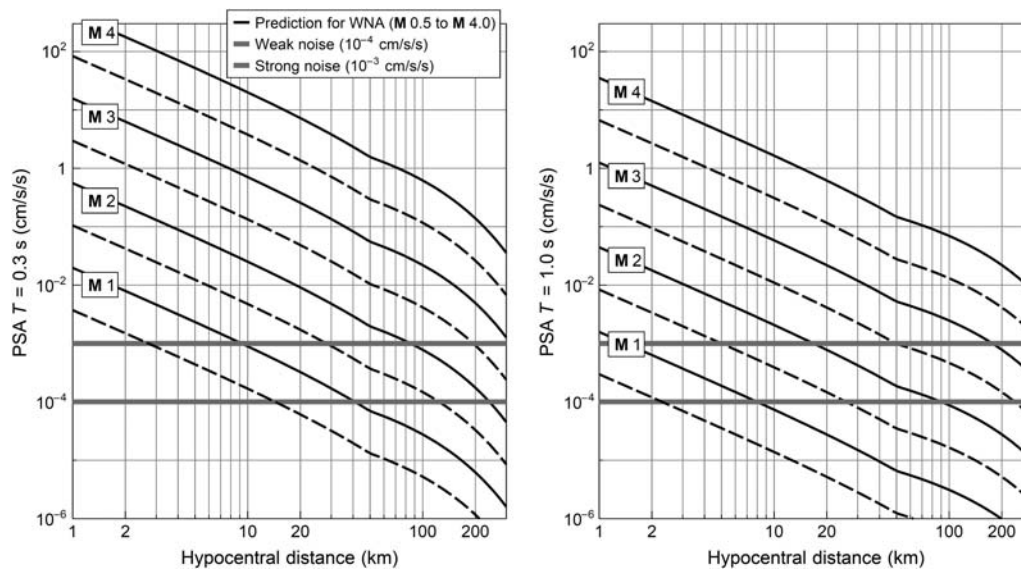


▲ **Figure 6.** Assessment of M estimates (equation 2) based on the ground motions from ENA database, showing the M bias determined for each record, as a function of hypocentral distance for three magnitude ranges (a–c). Mean bias is computed over all magnitudes at equal distance intervals of 20 km. (d) The average M estimate and its known value for earthquakes having three or more observations at $R \leq 300$ km. The solid line represents $M_{i,predicted} = M_{i,known}$, and the dashed lines indicate ± 0.1 band about the solid line.

the event should be recalculated using the 0.3 s PSA. We tested to confirm that there is no significant difference, on average, between M computed from 0.3 s or 1 s for M 3–4 events in the NGA-W2 and ENA databases, though the M value determined for individual events may vary by ± 0.13 units (standard deviation), depending on which ground-motion parameter is selected. More generally, we also investigated whether there is an advantage to using an average of M from the two ground-motion parameters for events in the intermediate-magnitude range of M 3.0–3.5 and found that this also makes no difference—individual-event M values may vary slightly (± 0.1), but overall the bias and its variability are the same. We therefore would generally recommend using the 1 s PSA formula for the initial M calculation and switching to the 0.3 s PSA formula if the calculated M from 1 s PSA is less than 3.0.

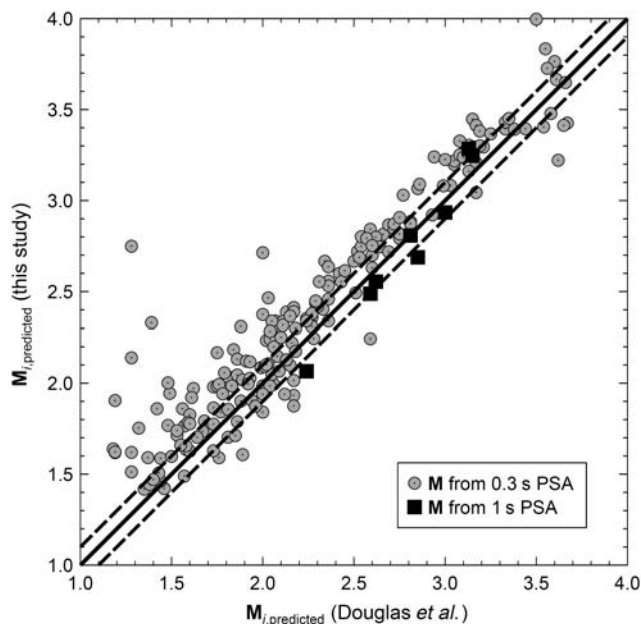
Ideally, we would like to be able to evaluate the performance of the algorithm for events as small as M 1, which is the threshold for some traffic light protocols. Small-magnitude ground-motion datasets with reliable moment magnitude esti-

mates are difficult to obtain, but a very good set was compiled by Douglas *et al.* (2013). They used ground-motion data from induced events, along with stochastic simulations, to develop a GMPE for induced earthquake ground motions in geothermal areas, including several areas in Europe and California. Their database of several thousand records contains events in the M 1–4 range, at close distances (< 50 km). Douglas *et al.* compiled horizontal-component PSA but corrected it for site conditions to an equivalent rock site condition, as characterized by a near-surface shear-wave velocity of 1100 m/s. Because of the correction to a reference rock condition, their horizontal-component amplitudes should be similar to those expected on the vertical component (e.g., see Siddiqi and Atkinson, 2002). Douglas *et al.* (2013) analyzed displacement spectral amplitudes in order to estimate moment magnitude for all events, as based on the Brune model. Atkinson (2014) shows that the observed ground-motion amplitudes for the Douglas database are well predicted by the stochastic simulation model for western events employed in this study. It is therefore reasonable



▲ **Figure 7.** Comparison of predicted PSA for WNA at (left) 0.3 s and (right) 1.0 s for events of M 0.5–4.0 versus hypocentral distance (black lines). Heavy gray horizontal lines show typical weak and strong noise levels.

to compare the magnitude estimation procedure proposed herein against the Douglas *et al.* database, assuming that the horizontal component, corrected for site effects, is equivalent to the vertical component. The comparison is shown in Figure 8 for events recorded by three or more stations. The magnitude calculations track each other well, but the moment




▲ **Figure 8.** Comparison of M estimated from PSA (this study) to M estimated from displacement spectra for the induced-seismicity ground-motion database of Douglas *et al.* (2013) for events recorded by three or more stations. The heavy solid line represents one-to-one match of magnitude estimates, and the dashed lines indicate ± 0.1 band about the solid line.

magnitudes calculated by our algorithm using 0.3 s PSA are on average 0.14 (± 0.20) units higher than those calculated by Douglas *et al.* (2013). There are many more data available in their database at 0.3 s (3300 records) than at 1 s (120 records), due to noise limitations, which further supports the switch to PSA at 0.3 s for $M < 3$ events. The agreement of average magnitude values within ~ 0.1 units is considered satisfactory, despite the significant variability in estimates from event to event. Thus, we believe the moment- M algorithm is robust down to at least M 1.5. We note on Figure 8 that there is a greater tendency toward overestimation of M for $M < 1.5$, likely due to noise effects on PSA.

For events of $M < 1.5$, our ability to determine magnitude will be limited by the station distribution and noise. If there are insufficient stations with clear signal-to-noise ratio (e.g., a factor of 3 or more over a significant frequency band), then the best that can be accomplished is to estimate an upper limit on the actual magnitude. For example, one might calculate M at each of the three closest stations (even if just barely above noise), all of which should be overestimates of the actual value of M , and estimate an upper limit on M as the average of these values. This strategy may be sufficient to establish that an event did not exceed a traffic light threshold such as M 1.

CONCLUSION

We have proposed a simple model (equation 2) to provide robust estimates of moment magnitude for $M < 4$ events, at distances less than ~ 300 km. The model can be refined on a regional basis as more detailed empirical information on the overall amplitude level and attenuation is gathered. The method is transparent and robust, being based on simple and well-known seismological scaling principles, and can be used in

typical network applications, as well as for traffic light systems for induced seismicity. 

ACKNOWLEDGMENTS

We thank Karen Assatourians, Behzad Hassani, Arpit Singh, and Sebastian Braganza for their help in compiling and processing datasets for the analyses. Financial support for this study was provided by the National Sciences and Engineering Research Council of Canada, TransAlta, and Nanometrics. We are grateful to Trevor Allen for constructive comments that improved the paper. We thank John Douglas for sharing his compiled data, and thanks go to the following for their permission to examine its components: Dirk Kraaijpoel (Koninklijk Nederlands Meteorologisch Instituut), Phillippe Jousset (International Centre for Geothermal Research, Potsdam), Vincenzo Convertito (Istituto Nazionale di Geofisica e Vulcanologia), and Ben Edwards (Eidgenössische Technische Hochschule Zürich).

REFERENCES

Anderson, J. G., and S. E. Hough (1984). A model for the shape of the Fourier amplitude spectrum of acceleration at high frequencies, *Bull. Seismol. Soc. Am.* **74**, 1969–1993.

Atkinson, G. (2012). Evaluation of attenuation models for the north-eastern U.S./southeastern Canada, *Seismol. Res. Lett.* **83**, 166–178.

Atkinson, G. (2014). Ground-motion prediction equation for small-to-moderate events at short hypocentral distances, with application to induced seismicity hazards, *Bull. Seismol. Soc. Am.* (submitted).

Atkinson, G., and A. Babaie Mahani (2013). Estimation of moment magnitude from ground motions at regional distances, *Bull. Seismol. Soc. Am.* **103**, 107–116.

Atkinson, G., and D. Boore (2006). Ground motion prediction equations for earthquakes in eastern North America, *Bull. Seismol. Soc. Am.* **96**, 2181–2205.

Atkinson, G., and D. Boore (2014). The attenuation of Fourier amplitudes for rock sites in eastern North America, *Bull. Seismol. Soc. Am.* **104**, 513–528.

Atkinson, G., and W. Silva (2000). Stochastic modeling of California ground motions, *Bull. Seismol. Soc. Am.* **90**, 255–274.

Atkinson, G., K. Assatourians, D. Boore, K. Campbell, and D. Motazedian (2009). A guide to differences between stochastic point-source and stochastic finite-fault simulations, *Bull. Seismol. Soc. Am.* **99**, 3192–3201.

Babaie Mahani, A., and G. Atkinson (2012). Regional differences in ground-motion amplitudes of small-to-moderate earthquake across North America, *Bull. Seismol. Soc. Am.* **103**, 2604–2620.

Boore, D. (1983). Stochastic simulation of high-frequency ground motions based on seismological models of the radiated spectra, *Bull. Seismol. Soc. Am.* **73**, 1865–1894.

Boore, D. (2003). Prediction of ground motion using the stochastic method, *Pure Appl. Geophys.* **160**, 635–676.

Boore, D. M. (2000). SMSIM—Fortran programs for simulating ground motions from earthquakes: version 2.0—A revision of OFR 96-80-A, *U.S. Geological Survey Open-File Rept. 2000-0509*, 55 pp.

Brune, J. (1970). Tectonic stress and the spectra of seismic shear waves from earthquakes, *J. Geophys. Res.* **75**, 4997–5009.

Campbell, K. (2009). Estimates of shear-wave Q and κ_0 for unconsolidated and semiconsolidated sediments in eastern North America, *Bull. Seismol. Soc. Am.* **99**, 3192–3201.

Douglas, J., B. Edwards, V. Convertito, N. Sharma, A. Tramelli, D. Kraaijpoel, B. Mean Cabrera, N. Maercklin, and C. Troise (2013). Predicting ground motion from induced earthquakes in geothermal areas, *Bull. Seismol. Soc. Am.* **103**, 1875–1897.

Hanks, T., and H. Kanamori (1979). A moment magnitude scale, *J. Geophys. Res.* **84**, 2348–2350.

Lermo, J., and F. Chavez-Garcia (1993). Site effect evaluation using spectral ratios with only one station, *Bull. Seismol. Soc. Am.* **83**, 1574–1594.

Raoof, M., R. Herrmann, and L. Malagnini (1999). Attenuation and excitation of three-component ground motion in southern California, *Bull. Seismol. Soc. Am.* **89**, 888–902.

Siddiqi, J., and G. Atkinson (2002). Ground motion amplification at rock sites across Canada, as determined from the horizontal-to-vertical component ratio, *Bull. Seismol. Soc. Am.* **92**, 877–884.

Wald, D. J., V. Quitoriano, T. H. Heaton, H. Kanamori, C. W. Scrivner, and B. C. Worden (1999). TriNet “ShakeMaps”: Rapid generation of peak ground-motion and intensity maps for earthquakes in southern California, *Earthq. Spectra* **15**, 537–556.

Yenier, E., and G. Atkinson (2014). Equivalent point-source modeling of moderate-to-large magnitude earthquakes and associated ground-motion saturation effects, *Bull. Seismol. Soc. Am.* **104**, doi: 10.1785/0120130147.

Gail M. Atkinson
Emrah Yenier
Western University
London, Canada N6A 5B7
gmatkinson@aol.com
emrah.yenier@gmail.com

D. Wesley Greig
Nanometrics
250 Herzberg Rd.
Kanata, Ontario K2K 2A1
wesgreig@nanometrics.ca